Density functional studies of muonium in nitrogen aggregate containing diamond: the Mu_X centre

2009 J. Phys.: Condens. Matter 21 364211

(http://iopscience.iop.org/0953-8984/21/36/364211)

J. Phys.: Condens. Matter **21** (2009) 364211 (6pp) doi:10.1088/0953-8984/21/36/364211

Density functional studies of muonium in nitrogen aggregate containing diamond: the Mu_X centre

K M Etmimi, J P Goss, P R Briddon and A M Gsiea

School of Electrical, Electronic and Computer Engineering, Newcastle University, Newcastle Upon Tyne, UK

E-mail: J.P.Goss@ncl.ac.uk

Received 5 April 2009, in final form 11 June 2009
Published 19 August 2009
Online at stacks.iop.org/JPhysCM/21/364211

Abstract

Diamond has potential as a wide band-gap semiconductor with high intrinsic carrier mobility, thermal conductivity and hardness. Hydrogen is involved in electrically active defects in chemical vapour deposited diamond, and muonium, via muon spin spectroscopy, can provide useful characterization for the configurations adopted by H atoms in a crystalline material. We present the results of a computational investigation into the structure of the Mu_X centre proposed to be associated with nitrogen aggregates. We find that the propensity of hydrogen or muonium to chemically react with the lattice makes the correlation of Mu_X with nitrogen aggregates problematic, and suggest alternative structures.

(Some figures in this article are in colour only in the electronic version)

1. Introduction

In the past decade, the quality of single-crystal diamond grown from the gas phase has reached levels suitable for electronics [1]. However, the incorporation of hydrogen present in the growth gas leads to electrically active defects [2–8], and there is a need to improve the understanding of H-containing point defects in diamond.

Muonium is a pseudo-isotope of hydrogen made up from a positive muon and an electron. Muon-spin-relaxation (μSR) experiments are sensitive probes of structure, and have been highly successful in determining the properties of H in a wide range of materials [9–13]. For pure diamond, two μSR centres labelled normal and anomalous muonium relate to the tetrahedral interstitial site (Mu_T) and bond-centred site (Mu_{BC}), respectively. The former exhibits an entirely isotropic hyperfine interaction (3711 $\pm$ 21 MHz), whereas Mu_{BC} is comprised from a combination of a relatively small isotropic term, and an anisotropic term along [111] ($A_s = -205.7$ MHz, $A_p = 186.9$ MHz) [10]. At low temperatures, both Mu_T and Mu_{BC} are observed, but the relative concentration of Mu_{BC} increases between 350 and 800 K, explained by an activated transitions from Mu_T to a thermodynamically more stable Mu_{BC}.

Another impurity common in diamond is nitrogen. Under geological or high-temperature, high-pressure laboratory annealing, nitrogen migrates and forms aggregates, of which nearest-neighbour pairs (A-centres) and four N atoms surrounding a vacant site (B-centres) are particularly stable. Diamond containing aggregated N exhibits the Mu_X centre in μSR [14], but the structure of this has not been unambiguously identified. Mu_X exhibits less than axial symmetry, and the large, isotropic hyperfine interaction is indicative of a chemically non-bonded muonium configuration: the μSR spectra are fitted to hyperfine parameters of $A_s = 4158 \pm 1500$ MHz and $A_p = 248 \pm 13$ MHz. Note the large error bar for A_s.

Additional experimental studies indicate muonium interacts with H2/H3 nitrogen-vacancy complexes [15–17] produced under gamma-irradiation of type Ia natural diamond followed by an annealing stage [18]. Theoretically, hydrogen (or muonium) in H3 represents a highly stable structure with the hydrogen atom chemically attaching to one of the two carbon radical sites [5]. In material containing H2/H3, Mu_X is suppressed and the diamagnetic fraction increased, which is interpreted as the H2/H3 centres trapping the muonium [18].

In this paper we present the results of density functional simulations to assess the interpretation of the experimental

Table 1. Calculated hyperfine tensors of Mu_T and Mu_{BC} (MHz). f is the ratio of the isotropic hyperfine interaction for the defect to that for muonium in vacuum (4463 MHz).

	Mu_T		Mu_{BC}	
	A_s	f	A_s	A_p
This study	4000	0.90	−276	232
Experiment [10]	3711	0.831	−205.7	186.9

data in the formation of Mu_X as a complex of muonium with either an A-centre or a B-centre. We also comment on the interaction of muonium with H2/H3 and examine some alternative structures potentially significant in the identification of Mu_X.

2. Method

Density functional theory calculations using a generalized gradient approximation [19] are carried out using the AIMPRO code [20, 21]. Wave functions are expanded in atom-centred Gaussian basis functions [22] (22, 40 and 16 functions for C, N and H atoms, respectively), and the charge density fitted to plane-wave up to 300 Ha. The optimized structures for point defects are obtained by relaxing all atoms in supercells comprised from 216 host sites (simple-cubic lattice with lattice vectors of length $3a_0$). For platelet structures, supercells made up from 256 host sites in an orthorhombic configuration corresponding to lattice vectors $[220]a_0$, $[2\bar{2}0]a_0$ and $[004]a_0$, with the addition of 16 self-interstitials in the Humble form [23, 24]. To obtain total energies, the Brillouin-zone is sampled using the Monkhorst–Pack scheme [25] with a uniform mesh of $2 \times 2 \times 2$ special k-points. Core electrons are eliminated by using norm-conserving pseudo-potentials [26], and hyperfine interactions obtained by reconstructing the all-electron wave functions in the core region [4, 27]. The calculated hyperfine interactions for free muonium are obtained by simulating a muon in a periodic lattice of sufficiently large lattice spacing to ensure no significant interaction between muonium and its periodic images. In practice this is achieved in a simple-cubic lattice of side length 7.15 Å, being two diamond lattice constants. Diffusion barriers have been obtained by using the climbing nudged elastic band formalism [28, 29]. Electrical levels are obtained by reference to a marker system [30].

3. Results

To confirm the accuracy of the computational scheme we have first analysed the properties of muonium in the Mu_T and Mu_{BC} configurations.

3.1. Muonium in diamond

Muonium and hydrogen in diamond has been modelled extensively [31–42]. In line with this body of work, we find the T-site is 1.25 eV higher in energy than the bond-centred site, and that the reaction T → BC is activated by 0.6 eV. These values are consistent with previous experiment [10].

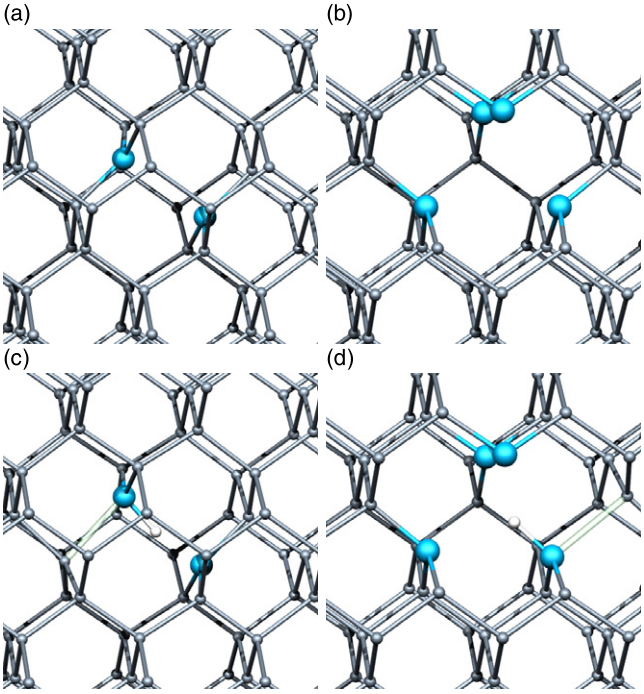

Figure 1. (Colour online) Schematics of (a) the A-centre, (b) the B-centre, (c) the A-centre–muonium complex, and (d) the B-centre–muonium complex in diamond. Vertical and horizontal directions are approximately [001] and [110] respectively. Small grey and white atoms are N and H/muonium, respectively, with large (blue) atoms showing the nitrogen sites. The transparent cylinders in (c) and (d) represent broken bonds relative to (a) and (b).

The calculated hyperfine tensors for the two sites are listed in table 1. Previous studies have suggested that vibrational motion of Mu_{BC} is important [43–45], and we have also estimated its impact. The resulting average reduces A_s by around 5%, and the anisotropic term by less than 1%. There is a 8% overestimate in value of A_s for Mu_T. However, this is somewhat mitigated if we consider the value relative to the calculated value for free muonium, which is also overestimated: if we refer the calculated value of A_s for Mu_T to the *calculated* value for muonium in vacuum rather than the experimental one, we get a value of $f = 0.86$, in closer agreement with experiment.

Most importantly in the context of the current study, there is a clear qualitative difference between Mu_T where the muonium is non-bonded and Mu_{BC} which chemically interacts. The error between modelling and experiment reported in table 1 are typical of hyperfine calculations [40], and we view the analysis of the A-tensors for Mu_T and Mu_{BC} to validate our method.

3.2. Muonium N-aggregate complexes

We have simulated the two model systems [14] for Mu_X: complexes of muonium with an A-centre or a B-centre. The resulting optimized structures are shown schematically in figure 1. It should be noted that both A- and B-configurations are particularly stable because all atoms are chemically satisfied. The addition of muonium (or hydrogen)

Table 2. Calculated hyperfine tensors of muonium complexes with A- and B-centres (MHz). The directions are indicate in spherical polar coordinates, θ degrees from the z-axis, and ϕ from the x-axis toward y in the xy-plane.

System	$\lvert A_1\rvert$	θ	ϕ	$\lvert A_2\rvert$	θ	ϕ	$\lvert A_3\rvert$	θ	ϕ
A-centre–μ	−25	90	−45	3	20	45	95	110	45
B-centre–μ	−92	90	135	−56	24	45	24	114	45

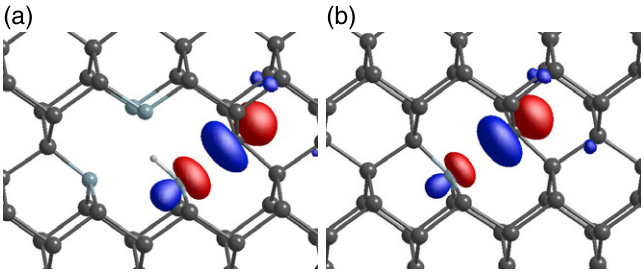

Figure 2. (Colour online) Unpaired electron Kohn–Sham functions for (a) B-centre–muonium complex and (b) neutral substitutional nitrogen (P1 EPR centre). Orientation is as in figure 1.

therefore may be expected to result in the chemical passivity being interrupted.

Experiment shows that Mu_X has a large isotropic hyperfine interaction, the same order of magnitude as Mu_T and free muonium, accompanied by a small anisotropic term not aligned to a crystal axis. Therefore, if a complex of an A-centre or B-centre with muonium is a candidate for Mu_X, it must not have axial symmetry, and most probably will not involve a covalent bond between the muonium and any other atom.

However, this is not what we find. In both cases, even where the muonium is initially placed in a non-bonding site in the environment of the N-aggregates, there is a *spontaneous chemical reaction* resulting in the production of a carbon radical some distance from the muon. The equilibrium structures for A-muonium and B-muonium complexes are shown in figures 1(c) and (d), respectively. Consistent with a chemical reaction, we find zero-temperature binding energies relative to dissociation into the N-aggregate and interstitial hydrogen/muonium for these complexes of 1.2 and 2.2 eV, which is in line with the notion of N-aggregates acting as deep muonium traps in N-containing diamond [14].

The spin density is strongly localized in the vicinity of the carbon radical sites, leading to small, highly anisotropic hyperfine tensors for the muon, as listed in table 2. They are therefore completely inconsistent with Mu_X. To illustrate the origin of the small hyperfine interaction at the muon, we show a plot of the localization of the unpaired electron for the B-centre–muonium complex in comparison to the well known P1 EPR centre which is chemically analogous (figure 2). In the case of the P1 EPR centre, the amount of spin density on the N-site is relatively small [46], and therefore the small values for the hyperfine interactions for muonium can be readily understood.

Noting that Mu_T is a metastable configuration, it is possible that muonium may locate at a metastable site within or close to an A-or B-centre. Therefore we have also obtained the hyperfine interactions for a muonium–B-centre complex where the muonium is constrained to not chemically react with the lattice. For one case, the muonium is fixed by symmetry to lie at the centre of the B-centre, and the second approximately at an T-site neighbouring the N-aggregate. Where muonium is centred in the core of the B-centre and a T_d symmetry constraint applied, there is a repulsive electrostatic interaction between the high electron density associated with the lone-pairs and that in the muonium. Consequentially the orbital containing the unpaired spin is driven up in energy relative to the case of Mu_T where there is a much lower electron-repulsion. In our simulations the unpaired electron becomes delocalized (effectively the centre auto-ionises and the electron lies in the conduction band), resulting in the small entirely isotropic hyperfine interaction of just 86 MHz.

In contrast, for a non-bonded muonium in an interstitial cage neighbouring the B-centre, the electronic structure and localization is practically indistinguishable from Mu_T, resulting in a calculated value of $A_s = 3962$ MHz. Similar results are obtained for muonium in the vicinity of an A-centre.

Substitutional nitrogen in diamond has a deep donor level at $E_c - 1.7$ eV [47], whereas A-centres have a donor level close to the valence band [48] and B-centres are thought to be electrically inactive [30]. We find that addition of hydrogen/muonium in A- and B-centres (in their equilibrium configurations, figure 1) produce deep donor levels. Using the donor level of substitutional N as a marker [22], the donor levels are $E_c - 0.9$ eV and $E_c - 1.1$ eV respectively for A-centre–muonium and B-centre–muonium. Note, the structural relaxation we find for the A-centre–muonium centre leads to a *deep* level rather than the shallow level previously proposed [49]. However, in the previous study, the shallow level corresponds to an on-axis structure which we find to be only metastable.

3.3. Muonium in nitrogen-vacancy complexes

The H2/H3 centre is made up from an A-centre trapping a lattice vacancy. H2 and H3 are labels for optical transitions, which are associated with the negative and neutral charge states, respectively. The stability of hydrogen in H3 centre has been studied theoretically [30] and recent μSR suggests a strong muonium interaction with these centres [18]. The calculations yield a single clear minimum energy structure where hydrogen/muonium is bonded to one carbon atom to tie off a dangling bond. In the neutral charge state the unpaired spin is strongly localized on the remaining carbon radical site in the vacancy, and as a consequence of the localization the hyperfine tensor on the H/muon site is small: −62 MHz along $[1\bar{1}0]$, −49 MHz at 8° from [001] and 90 MHz at 8° from [110]. In the negative charge state N_2VH is EPR-inactive. In agreement with the interpretation of the experiment, an H2/H3 centre would be expected to be a deep trap for muonium or hydrogen with a zero-temperature binding energy of around 6 eV for both neutral and negative charge states.

Table 3. Calculated hyperfine tensors for muonium in a range of model cavities (MHz). f and f' are ratios of A_s to the experimental and calculated values for free muonium, respectively. The experimental values for Mu_X are shown for comparison.

Model cavity	A_s	f	f'	A_p
V_1N_4	86	0.02	0.02	0
V_2N_6	4388	0.98	0.94	−12
V_5N_{12}	4650	1.04	1.00	0
V_8N_{18}	4695	1.05	1.01	1
Mu_X	4158	0.93	—	248

3.4. Muonium in other sites

Simulations of N-aggregates and muonium have all resulted in exothermic chemical reactions, leading to carbon radical sites and small, highly anisotropic hyperfine interactions with the muons.

There remains the possibility that the Mu_X centre is not associated with the N-aggregates directly. In type Ia material there are other candidate structures. In particular, such diamonds also contain nano-cavities (aggregates of lattice vacancies) and platelets thought to be made up from planar self-interstitial aggregates [23, 24, 50].

Both have open regions that may trap the mobile muonium, and that would result in large isotropic components to the hyperfine interaction, consistent with the measured values for Mu_X.

To simulate nano-cavities we have removed one, two, five and eight carbon atoms in symmetric arrangements. The remaining under-coordinated carbon sites are replaced by nitrogen to produce a chemically passive void in the diamond lattice. The question we specifically address is not whether these voids are responsible for Mu_X, but to assess how large a cavity might need to be to achieve an isotropic component of the hyperfine tensor on the muonium as large as observed in experiment. The values for the hyperfine tensors where the muonium is fixed at the centre of the voids are listed in table 3. We note that the theoretical ratio, of isotropic terms, f', for a divacancy is the best agreement with the experimental ratio, f, for Mu_X, and larger voids result in muonium indistinguishable, at least in our calculations, from free muonium.

The stability of these non-bonded structures requires some discussion. Hydrogen/muonium in V_2N_6 cavity has many metastable configurations, including the non-bonded case, and several chemically reacted forms similar structure to that seen for the B-centre (figures 1(d) and 2(a)). We noted above that the reaction of hydrogen/muonium with the A- and B-centres are spontaneous, i.e. there is no barrier. In the case of the larger N-terminated cavities the situation is closer to that for Mu_T, and a barrier exists for a chemical reaction between the muonium and the lattice. For V_2N_6 this activation energy is calculated to be 0.4 eV, and the reaction is exothermic by 1.2 eV. The chemically reacted forms all have hyperfine interactions at the muonium site which are small and highly anisotropic.

Perhaps a more favourable option for the site of Mu_X would be the self-interstitial platelet, as this has a reasonably regular structure that may be expected to yield a non-axial

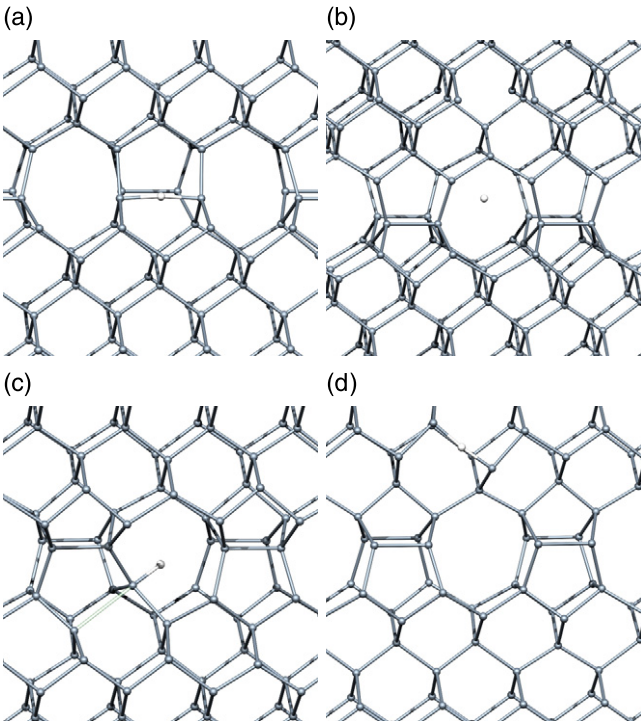

Figure 3. Schematics showing selected structures of muonium in the platelet defect. The grey and white atoms are carbon and muonium, respectively. Vertical and horizontal directions are approximately [001] and [110] respectively.

Table 4. Calculated hyperfine tensors for muonium in a model platelet, (MHz), for the structures presented in figure 3.

Structure	A_s	A_p	Principal direction
(a)	−289	157	[110]
(b)	4594	1	[001]
(c)	367	5	[111]
(d)	−278	230	$[11\bar{1}]$

tensor. Figure 3 shows four characteristic structures, where the combinations of five, six and eight member rings are generated by the planar agglomeration of tetra-interstitials [23, 24]. The lowest energy is found where muonium forms a three-centre bond between two carbon atoms that make up a next-neighbour reconstruction in the pure carbon platelet (figure 3(a)). The unpaired electron is highly localized and yields a muon hyperfine tensor more characteristic of Mu_{BC} than of Mu_X (see table 4).

However, in a form reminiscent of Mu_T there is a metastable configuration where muonium resides in the open channel produced by the platelet, as shown in figure 3(b). The hyperfine tensor for this structure is much closer in nature to Mu_X. However, the stability of this site is marginal, and it tends to react with neighbouring carbon to form an anti-bonding configuration close in energy, shown in figure 3(c), which does not yield agreement with the hyperfine interactions of Mu_X.

However, the zero-point motion of a muonium species in the channel is expected to be appreciably large. We

have estimated the difference in zero-point energy between chemically bonded and non-bonded muonium in diamond to be of the order of 0.2–0.3 eV, comparable to the energy difference between configurations (b) and (c). If, when vibrational terms are included, the non-bonded form is more stable than (c), then it is possible that the Mu_X centre is associated with non-bonded muonium in platelets. In real diamonds, platelet structures are disordered, with nitrogen incorporated, and the amount of relaxation affected by the platelet size [51–54]. This variability in sites within the platelet may relate to the uncertainty in the isotropic component of the hyperfine interaction reported for Mu_X.

Finally, we note that there are many other metastable structures for muonium chemically incorporated into the platelet. All of these structures introduce deep electrical levels similar to bond-centred hydrogen, and hyperfine tensors close to Mu_{BC}. In addition, the energy for the case where the muonium is sited just outside of the platelet core (figure 3(d)) is 2.3 eV higher than the lowest energy state we found within the structure, showing how the platelets represent trapping sites for hydrogen or muonium.

4. Discussion and conclusions

The small, anisotropic calculated hyperfine tensors for the ground-state configurations of complexes of muonium with A- and B-centres mean that these centres are most probably not responsible for Mu_X. However, this interpretation must be viewed in the context of a number of issues.

First it has been suggested that some of the error in the estimate of the hyperfine tensor for anomalous muonium arises from the zero-point motion of the very light muon along the axis of the C–C bond [43–45]. Could zero-point motion for either of the complexes result in agreement with the Mu_X parameters? We view this as unlikely since even in the case of Mu_{BC} the effect of including motional averaging is a small perturbation, whereas for either the A-centre–muonium or B-centre–muonium complexes the isotropic term must increase by two orders of magnitude to match the measured values of Mu_X.

A second possibility is that Mu_X results from muonium in a region not directly within the N-aggregates, but in an approximately tetrahedral cage in the immediate vicinity of them. However, as indicated in section 3, the perturbation to the hyperfine tensors of Mu_T even in the T-sites immediately adjacent to the A- and B-centres is very small. Coupled with the small binding energies in these chemically unreacted sites and barrier-less reactions to form carbon radicals, it is not clear how near-by structures might be responsible for Mu_X, but it remains a possibility given the large uncertainty in the experimental parameters.

A final possibility is that muonium is tunnelling rapidly between sites around the N-aggregates. Indeed, such effects are thought to be present in the case of muonium in Zn-doped GaAs [55], but if this were the case in N-containing diamond, it is not obvious why the resulting hyperfine tensor would be non-axial given the high symmetry of the two nitrogen aggregates involved.

If Mu_X is not associated directly with A-or B-centres, then a possible explanation is that Mu_X is related to different centre also present in type Ia diamond. Small voids yield hyperfine tensors close to muonium in vacuum, and possess barriers to chemical reactions. However, it is unclear how to explain the anisotropic component in such a model, and there is relatively little evidence for small, chemically passive voids. In contrast, the evidence for the presence and structure of platelets in Ia diamond containing B-centres is quite clear. Based upon our calculations a possible configuration for muonium within the open channels of the platelets also has some merit, but again the identification of the anisotropic term may be problematic.

In summary, although none of the models examined for Mu_X is a particularly good fit, the calculations show that a simple configuration made up from an A-centre–muonium or B-centre–muonium complex is unlikely to be responsible. To further investigate a potential role for the platelet, it would be beneficial to explore the presence of Mu_X in material containing only A-centres. If a direct interaction is taking place between muonium and A- and/or B-centres, we would expect to see a centre with a small, isotropic hyperfine interaction with the muon.

References

[1] Isberg J, Hammersberg J, Johansson E, Wikström T, Twitchen D J, Whitehead A J, Coe S E and Scarsbrook G A 2002 *Science* **297** 1670–2

[2] Glover C, Newton M E, Martineau P, Twitchen D J and Baker J M 2003 *Phys. Rev. Lett.* **90** 185507

[3] Glover C, Newton M E, Martineau P M, Quinn S and Twitchen D J 2004 *Phys. Rev. Lett.* **92** 135502

[4] Shaw M J, Briddon P R, Goss J P, Rayson M J, Kerridge A, Harker A H and Stoneham A M 2005 *Phys. Rev. Lett.* **95** 105502

[5] Goss J P, Briddon P R, Jones R and Sque S 2003 *J. Phys.: Condens. Matter* **15** S2903–11

[6] Kerridge A, Harker A H and Stoneham A M 2004 *J. Phys.: Condens. Matter* **16** 8743–51

[7] Iakoubovskii K, Stesmans A, Suzuki K, Sawabe A and Yamada T 2002 *Phys. Rev.* B **66** 113203

[8] Edmonds A M, Newton M E, Martineau P M, Twitchen D J and Williams S D 2008 *Phys. Rev.* B **77** 245205

[9] Cox S F J and Lichti R L 1997 *J. Alloys Compounds* **253** 414–9

[10] Holzschuh E, Kündig W, Meier P F, Patterson B D, Sellschop J P F, Stemmet M C and Appel H 1982 *Phys. Rev.* A **25** 1272–86

[11] Lichti R L, Cox S F J, Chow K H, Davis E A, Estle T L, Hitti B, Mytilineou E and Schwab C 1999 *Phys. Rev.* B **60** 1734–45

[12] Cox S F J and Symons M C R 1986 *Chem. Phys. Lett.* **126** 516–25

[13] Cox S F J 2003 *J. Phys.: Condens. Matter* **15** R1727–80

[14] Machi I Z, Connell S H, Baker M, Sellschop J P F, Bharuth-Ram K, Fischer C G, Nilen R W, Cox S F J and Butler J E 2000 *Physica* B **289/290** 507–10

[15] Mita Y, Nisida Y, Suito K, Onodera A and Yazu S 1990 *J. Phys.: Condens. Matter* **2** 8567–74

[16] Lawson S C, Davies G, Collins A T and Mainwood A 1992 *J. Phys.: Condens. Matter* **4** 3439–52

[17] Jones R, Torres V J B, Briddon P R and Öberg S 1994 *Mater. Sci. Forum* **143–147** 45–50

[18] Machi I Z, Connell S H, Sellschop J P F and Bharuth-Ram K 2001 *Hyperfine Interact.* **136/137** 727–30

[19] Perdew J P, Burke K and Ernzerhof M 1996 *Phys. Rev. Lett.* **77** 3865–8

[20] Briddon P R and Jones R 2000 *Phys. Status Solidi* b **217** 131–71

[21] Rayson M J and Briddon P R 2008 *Comput. Phys. Commun.* **178** 128–34
[22] Goss J P, Shaw M J and Briddon P R 2007 *Theory of Defects in Semiconductors* (*Topics in Applied Physics* vol 104) ed D A Drabold and S K Estreicher (Berlin: Springer) pp 69–94
[23] Humble P 1982 *Proc. R. Soc.* A **381** 65–81
[24] Goss J P, Coomer B J, Jones R, Fall C J, Briddon P R and Öberg S 2003 *Phys. Rev.* B **67** 165208
[25] Monkhorst H J and Pack J D 1976 *Phys. Rev.* B **13** 5188–92
[26] Hartwigsen C, Goedecker S and Hutter J 1998 *Phys. Rev.* B **58** 3641–62
[27] Blöchl P E 1994 *Phys. Rev.* B **50** 17953–79
[28] Henkelman G, Uberuaga B P and Jónsson H 2000 *J. Chem. Phys.* **113** 9901–4
[29] Henkelman G and Jónsson H 2000 *J. Chem. Phys.* **113** 9978–85
[30] Goss J P, Briddon P R, Sque S J and Jones R 2004 *Diamond Relat. Mater.* **13** 684–90
[31] Sahoo N, Mishra S K, Mishra K C, Coker A, Das T P, Mitra C K, Snyder L C and Glodeanu A 1983 *Phys. Rev. Lett.* **50** 913–7
[32] Mainwood A and Stoneham A M 1984 *J. Phys. C: Solid State Phys.* **17** 2513–24
[33] Estreicher S, Ray A K, Fry J L and Marynick D S 1985 *Phys. Rev. Lett.* **55** 1976–8
[34] Claxton T A, Evans A and Symons M C R 1986 *J. Chem. Soc. Faraday Trans.* **82** 2031–7
[35] Estle T L, Estreicher S and Marynick D S 1986 *Hyperfine Interact.* **32** 637–9
[36] Estreicher S, Ray A K, Fry J L and Marynick D S 1986 *Phys. Rev.* B **34** 6071–9
[37] Estle T L, Estreicher S and Marynick D S 1987 *Phys. Rev. Lett.* **58** 1547–50
[38] Briddon P, Jones R and Lister G M S 1988 *J. Phys. C: Solid State Phys.* **21** L1027–31
[39] Goss J P, Jones R, Heggie M I, Ewels C P, Briddon P R and Öberg S 2002 *Phys. Rev.* B **65** 115207
[40] Goss J P 2003 *J. Phys.: Condens. Matter* **15** R551–80
[41] Ramirez R, Herrero C P and Hernandez E R 2006 *Phys. Rev.* B **73** 245202
[42] Herrero C P and Ramirez R 2007 *Phys. Rev. Lett.* **99** 205504
[43] Chawla S and Messmer R P 1996 *Appl. Phys. Lett.* **69** 3251–53
[44] Bendazzoli G L and Donzelli O 1989 *J. Phys.: Condens. Matter* **1** 8227–34
[45] Paschedag N, Suter H U, Maric Dj M and Meier P F 1993 *Phys. Rev. Lett.* **70** 154–7
[46] Smith W V, Sorokin P P, Gelles I L and Lasher G J 1959 *Phys. Rev.* **115** 1546–53
[47] Farrer R 1969 *Solid State Commun.* **7** 685
[48] Davies G 1976 *J. Phys. C: Solid State Phys.* **9** L537–42
[49] Miyazaki T, Okushi H and Uda T 2002 *Phys. Rev. Lett.* **88** 066402
[50] Goss J P, Briddon P R, Jones R and Heggie M I 2006 *Phys. Rev.* B **73** 115204
[51] Berger S D and Pennycook S J 1982 *Nature* **298** 635–7
[52] Fallon P J, Brown L M, Barry J C and Bruley J 1995 *Phil. Mag.* A **72** 21–37
[53] Bruley J 1992 *Phil. Mag. Lett.* **66** 47–56
[54] Clackson S G, Moore M, Walmsley J C and Woods G S 1990 *Phil. Mag.* B **62** 115–28
[55] Chow K H, Hitti B, Keifl R F, Lichti R L and Estel T L 2001 *Phys. Rev. Lett.* **87** 216403